J Solid State Eletrochem (2003) 8: 73–78
DOI 10.1007/s10008-003-0397-5

ORIGINAL PAPER

Y. P. Wu · R. Holze

Anode materials for lithium ion batteries obtained by mild and uniformly controlled oxidation of natural graphite

Received: 15 November 2002 / Accepted: 11 June 2003 / Published online: 27 September 2003

Abstract Modification of natural graphite for anode materials has been a recent focus of research and development. Here we report that a common natural graphite, whose electrochemical performance is very poor, can be modified by solutions of $(NH_4)_2S_2O_8$, concentrated nitric acid solution, or green chemical solutions such as aqueous solutions of hydrogen peroxide and ceric sulfate. All treatments result in marked improvement of the electrochemical performance, including reversible capacity, coulombic efficiency in the first cycle, and cycling behavior. The main reason is the effective removal of active defects in natural graphite, formation of a new dense surface film consisting of oxides, improvement of the graphite stability, and introduction of more nanochannels/micropores. As a result, these changes inhibit the decomposition of electrolytes, prevent the movement of graphene planes along the *a*-axis direction, and provide more passages and storage sites for lithium. They are mild and the uniformity of the product can be well controlled. Pilot experiments show economic promise for their application in industry to manufacture anode materials for lithium ion batteries.

Keywords Anode material · Lithium ion battery · Mild oxidation · Natural graphite

Presented at the 3rd International Meeting on Advanced Batteries and Accumulators, 16–20 June 2002, Brno, Czech Republic

Y. P. Wu · R. Holze (✉)
Institut für Chemie, AG Elektrochemie,
Technische Universität Chemnitz,
09107 Chemnitz, Germany
E-mail: rudolf.holze@chemie.tu-chemnitz.de

Y. P. Wu
Division of Chemical Engineering,
INET, Tsinghua University,
102201 Beijing, China

Introduction

Since the birth of the lithium ion battery in the early 1990s, its development has been very rapid due to its many advantages over the traditional rechargeable battery systems such as high output voltage, light weight, high energy density, and long cycle life [1]. So far, a lot of anode materials has been studied, such as graphitic carbon, amorphous carbon from heat treatment at temperatures below 1200 °C, nitrides of lithium and transition metal elements, silicides, tin-based oxides, novel alloys, and carbon composites [1, 2]. However, to our knowledge, only graphitic carbon is commercially available, although there is a report of a carbon composite [3].

In the case of graphitic carbon, it requires heat treatment at a high temperature (3000 °C) in order to form a graphitic structure. During this process, undesirable gases such as CO_2, CO, and C_xH_y are formed in combination with high energy consumption. In contrast, natural graphite already has a graphitic structure, and thus does not require high-temperature heat treatment. In addition, it is cheap and easily and abundantly available. Consequently, research on the modification of natural graphite has recently become a focus of attention [4, 5, 6, 7, 8, 9, 10, 11]. However, material properties, including crystal parameters such as the interlayer distance d_{002}, the crystal size L_c and L_a, sources, and processing will result in differences in electrochemical performance.

Recently, we found that a common natural graphite from China could be modified by air oxidation in the temperature range 500–700 °C [12, 13]. The main finding is that the defects that cause deterioration of the electrochemical performance can be removed by this treatment. As a result, the electrochemical behavior as an anode material for lithium ion batteries has been markedly improved. However, this process happens in a gas-solid interphase reaction, and the uniformity is not well controlled. For application in industry, mild and

uniformly controlled methods are preferred. In the investigation reported here, we found that solutions of strong oxidants could meet this demand.

Experimental

Natural graphite (Beishu Graphite Plant, China, designated as A) with $d_{002} = 3.351$ Å and $L_c = 120$ Å was initially soaked in an aqueous solution of KOH to remove mineral constituents. Subsequently, it was dipped into a 0.1 mol/L aqueous solution of $(NH_4)_2S_2O_8$ and 1 mol/L of H_2SO_4 at $T = 20$, 60, 100, and 120 °C, separately, then washed with water until the eluent was neutral, and finally dried. The prepared products were marked LS1, LS2, LS3, and LS4, respectively.

In the case of concentrated nitric acid solution as oxidant, natural graphite A was dipped into this solution under stirring at $T = 20$, 60, and 100 °C, separately, subsequently washed with water until neutral, and dried. The prepared products were marked N1, N2, and N3, respectively.

When an aqueous solution of 1 M H_2O_2 or a saturated solution of $Ce(SO_4)_2$ were used as oxidants, natural graphite was dipped into them with subsequent heating to 60 °C, followed by rinsing with water and drying. The dried products were marked A1 and A2, respectively.

X-ray photoelectron spectra (XPS) were obtained with an ES-300 spectrometer (Kratos, Japan). The relative O and C contents at the surface of the natural graphite were calculated on the basis of their photoionization cross sections and the integrals of their X-ray photoelectron intensities. Electron paramagnetic resonance spectra (EPR) were acquired with an EPR-200 spectrometer (Bruker, Germany). Thermogravimetry and differential thermal analysis (TG-DTA) were performed with a PCT-1 instrument under air (Beijing Analytical Instruments, China); the heating rate was 20 °C/min. High-resolution electron micrographs (HREM) were recorded with a JEM-200CX microscope (Jeol, Japan). Samples were uniformly pre-dispersed on micro-nets with cavities of micrometer size. FT-IR spectra were obtained with a Nicolet 560 spectrometer with samples dried under vacuum prior to the measurement (Thermo Electron, USA). BET surface areas were measured with an ST-03 instrument through nitrogen sorption and desorption (Beijing Analytical Instruments, China). Distribution of particle (DPA) sizes was obtained with a SA-CP3 particle size analyzer (Shimadzu, Australia/New Zealand), and the outer specific surface areas were calculated assuming that the particles were spherical. Capacity and cycling behavior were tested by a method reported elsewhere [13], which used lithium foils as the counter and reference electrodes and a solution of 1 mol/L $LiClO_4$ in a mixture of EC/DEC (v/v = 3:7) as the electrolyte and a homemade porous PP film as a separator. The anode was prepared by pressing the mixture of natural graphite and 5 wt% PVDF binder dissolved in N,*N*′-dimethylformamide into pellets with a diameter of ca. 1 cm. After drying under vacuum at 120 °C overnight, the anode pellets were put into an argon box and assembled into model cells under humidity of < 200 ppm. Electrochemical performance was measured galvanostatically at 0.2 mA with a CT2001A cell test instrument (Wuhan Land Electronic, China) for discharge (intercalation process) and charge (deintercalation process); the voltage ranged from 0.0 to 2.0 V versus Li^+/Li.

Results and discussion

Solution of $(NH_4)_2S_2O_8$ as oxidant

It is known that there are many structural imperfections such as sp^3 hybridized carbon atoms, edge carbon atoms, and carbon chains in graphite [14, 15], especially in natural graphite, due to its incomplete graphitization during the natural formation process. These structures are prone to oxidative removal during reaction with a solution of $(NH_4)_2S_2O_8$, which has a very strong oxidative capability. Consequently, the surface structure of the natural graphite A is changed after the oxidation treatment. XPS spectra of O_{1s} in the samples A and LS2 are shown in Fig. 1 and selected results are summarized in Table 1.. They indicate that oxygen atoms are present in four kinds of species before and after oxidation, i.e. hydroxyl/phenolic oxygen, ether oxygen, carboxylic oxygen in COOR (R = H and alkyl), and carbonyl oxygen in acetone/quinone, corresponding to binding energy peaks at 534.1, 533.2, 532.3, and 530.9 eV, respectively [16, 17].

X-ray photoelectron spectra of C_{1s} in the samples A and LS2 are shown in Fig. 2; selected data are also summarized in Table 1. Four kinds of carbon atoms species are present, i.e. carbonyl carbon in acetone/quinone, carboxylic carbon in COOR (R = H and alkyl),

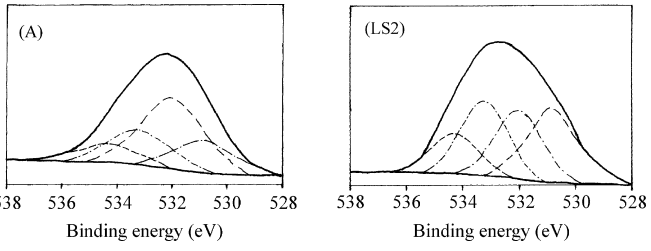

Fig. 1 XPS spectra of O_{1s} at the surface of natural graphite before (A) and after oxidation treatment (LS2)

Table 1 Experimental data of natural graphite before (A) and after (LS1, LS2, LS3 and LS4) oxidation with a solution of $(NH_4)_2S_2O_8$

Sample	Treatment temperature (°C)	Weight loss (%)	Atomic ratio of O at the surface (%)	Atomic ratio of C at the surface (%)	Species and percentage of oxygen atoms				Species and percentage of carbon atoms			
					534.1 eV	533.2 eV	532.3 eV	530.9 eV	288.9 eV	287.2 eV	285.9 eV	284.4 eV
A	–	–	4.11	95.89	0.1268	0.2320	0.4526	0.1886	0.0299	0.0534	0.1029	0.8138
LS1	20	2.64	4.70	95.30	0.1563	0.2651	0.3242	0.2544	0.0367	0.0575	0.0837	0.8221
LS2	60	2.07	6.03	93.97	0.1538	0.2834	0.2563	0.3065	0.0353	0.0641	0.1449	0.7556
LS3	100	1.83	5.95	94.05	0.1020	0.2800	0.3933	0.2247	0.0337	0.0441	0.0973	0.8249
LS4	120	1.67	5.33	94.67	0.1621	0.3251	0.3567	0.1560	0.0300	0.0717	0.1396	0.7587

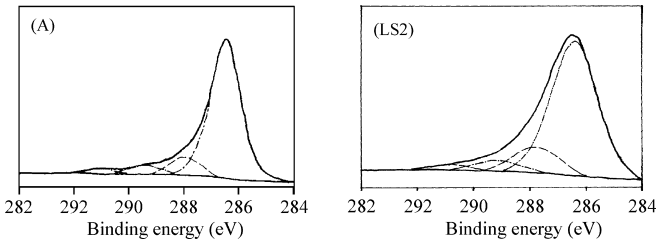

Fig. 2 XPS spectra of C_{1s} at the surface of natural graphite before (A) and after oxidation treatment (LS2)

ether/phenolic carbon in C-O-C and C-OH, and carbon atoms in graphene planes, corresponding to binding energies at 288.9, 287.2, 285.9, and 284.4 eV, respectively [16, 17].

As already noted, virgin natural graphite A was initially treated in a KOH solution to remove minerals. As a result, four kinds of oxygen and carbon atoms were also observed, as with samples from subsequent oxidation. Based on the data collected in Table 1, no unequivocal evidence indicating which kind(s) of compound(s) was(were) involved by oxidation with $(NH_4)_2S_2O_8$ is available. A conceivable reason is the presumably complicated oxidation reaction. However, the weakly adsorbed oxygen atoms were removed and replaced by a new layer of oxides formed during the oxidation and bonded more firmly to the carbon structure [18], because the results in Table 1 show that the oxygen atom content at the surface increased from 4.11% to 4.70, 6.03, 5.95, and 5.33%; in addition, there was a slight weight loss after the mild oxidation treatment: 2.64, 2.07, 1.83, and 1.67%.

FT-IR spectra of oxidized natural graphite LS2 were obtained using natural graphite A as the reference sample (Fig. 3). A few absorption bands, especially of surface oxygen-including groups, were identified, apparently consistent with the results from XPS and in particular with the observed increase in surface oxygen content. A very strong band centered at 3451 cm^{-1} is assigned to $\nu_{(O\text{-}H)}$ of alcoholic/phenolic groups. The band at 1741 cm^{-1} is characteristic of the stretching mode of carbonyl groups, $\nu_{(C=O)}$, and the one at 1637 cm^{-1} is due to $\nu_{(C=O)}$ of quinones.. The band at 1371 cm^{-1} may be assigned to $\delta_{(O\text{-}H)i.p.}$ of esters. Around 1000 cm^{-1} there is a wide weak band corresponding to $\nu_{as(C\text{-}O\text{-}C)}$ in ethers.

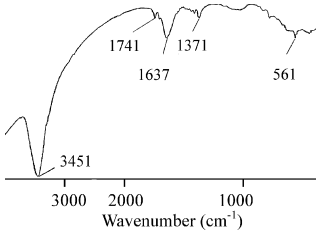

Fig. 3 FT-IR spectrum of the prepared natural graphite LS2 using natural graphite A as the reference sample

Since some reactive structural imperfections were eliminated, the structure of the prepared natural graphite became more stable. Curves for thermogravimetry and differential thermal analysis (TG-DTA) of A and the prepared natural graphite samples (LS1, LS2, and LS3) are shown in Fig. 4. At first, the weight decreased slowly because of the thermal decomposition of some oxides and slight oxidation. At temperatures above 500 °C, combustion began and the DTA curves increased. When the combustion reaction occurred rapidly, the DTA curves peaked. After the oxidation treatment of graphite A the exothermal peaks shifted from 742 to 761, 761, and 752 °C, respectively. Usually, defects are easily oxidized and initiate the combustion reaction of natural graphite at lower temperatures. After the removal of these active sites, the natural graphite structure became more stable, and the exothermal peaks shifted to higher temperatures, which is consistent with the discussion above, though the shift is small.

HREM micrographs of natural graphite A and LS1 are shown in Fig. 5, and indicate an increase in the number of micropores and nanochannels after mild oxidation. This increase should be reflected in the data for the surface area. However, the results from the BET measurement shown in Table 2 surprisingly indicate that the specific surface area determined with the BET method decreased after mild oxidation. It can be understood that reactive functional groups or defects at the graphite surface are oxidatively removed, resulting in a "smoother" surface and lower surface area. This seems to contradict at first glance the microscopic results, but both can be assumed to be correct. Additional data on the distribution of the particle diameters of natural

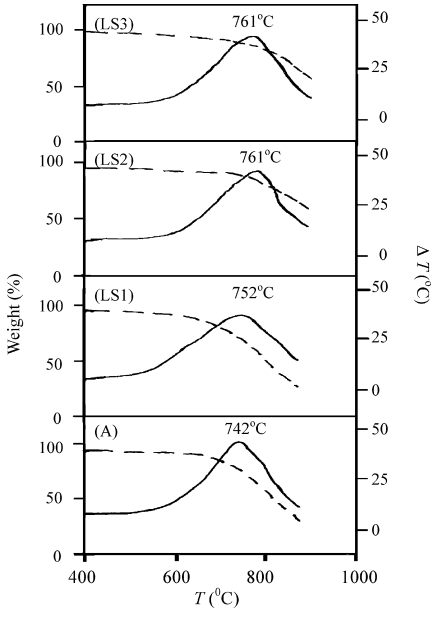

Fig. 4 TG-DTA curves of natural graphite before (A) and after (LS1, LS2, and LS3) oxidation treatment (*dashed lines*: TG curves; *full lines*: DTA curves)

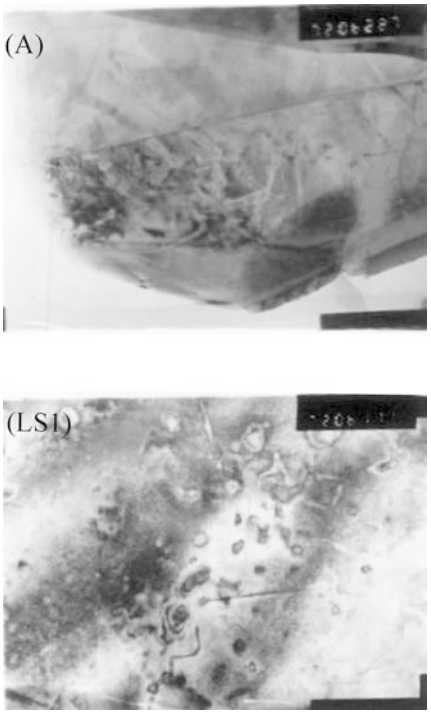

Fig. 5 HREM micrographs of natural graphite before (A) and after (LS1) oxidation treatment with width of 310 nm

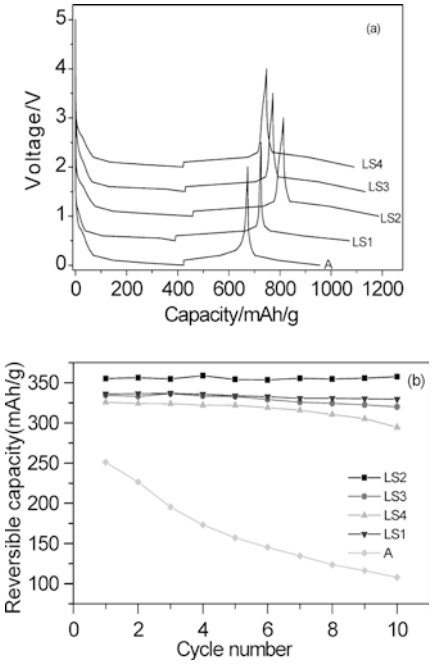

Fig. 6 (**a**) Discharge and charge profiles in the first cycle and discharge profiles in the second cycle and (**b**) cycling behavior of natural graphite A and the prepared samples LS1, LS2, LS3, and LS4 (in **a**, the voltages of LS1, LS2, LS3 and LS4 are shifted upwards by 0.5, 1.0, 1.5, and 2.0 V, respectively, for clarity)

graphite A and LS1 were measured in order to clarify this apparent inconsistency, and the outer specific surface area was calculated and is listed in Table 2.. From the difference, the internal specific surface area was calculated and is also listed in Table 2. This implies clearly that the internal surface area and, consequently, the number of micropores and nanochannels have increased after oxidation, which is also consistent with results from the oxidation of an activated carbon [18]. This result supports that HREM can image the change of micropores, i.e. the internal specific surface area, and the BET measurements reflect the total specific surface area.

Discharge and charge profiles in the first cycle and discharge profiles in the second cycle and cycling behavior of natural graphite A and the prepared samples LS1, LS2, LS3, and LS4 are presented in Fig. 6. As mentioned above, the electrochemical properties of the natural graphite without this treatment were poor. Its reversible capacity was only 251 mAh/g, the coulomb efficiency in the first cycle was 64%, and the reversible capacity faded to 100 mAh/g in the first 10 cycles. After modification, the reversible capacity increased to >350 mAh/g and the coulombic efficiency in the first cycle increased to $>85\%$. In the cases of LS1 and LS2, there was no evident fading in reversible capacity. In the cases of LS3 and LS4, there was a slight fading, but the performance was still much better than that of virginal graphite A. These improvements can be ascribed to the following reasons. (1) As mentioned above, some reactive structural imperfections were eliminated, and therefore the decomposition of electrolyte solvent molecules such as EC and DEC was less likely. (2) The graphite surface was covered with a fresh and dense layer of oxides, including hydroxyl/phenol, ether, ester, and carbonyl groups. This layer could act as a passivating film when lithium intercalated, and also hindered the decomposition of solvent molecules and the co-intercalation of solvated Li^+. (3) There is an increase in the number of micropores and nanochannels through the mild oxidation treatment to eliminate structural imperfections. It is well known that micropores can act as matrices for lithium storage in the form of lithium molecules or lithium clusters [19, 20]. In addition, micropores provide inlets and outlets for lithium during the discharge and charge processes, and favor lithium intercalation. (4) The graphite stability is increased; consequently, the movement of graphene planes around

Table 2 BET data and outer surface area data based on distribution of particle diameter (DPA) of natural graphite before (A) and after (LS1 and LS2) mild oxidation

Sample	Specific surface area from ET (m^2/g)	Outer specific surface area from DPA (m^2/g)	Calculated internal specific surface area (m^2/g)
A	5.34	1.229	4.11
LS1	5.09	0.623	4.37
LS3	4.92	–	–

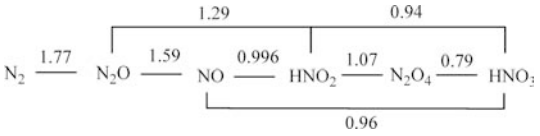

Scheme 1 Part of the standard oxidation–reduction potentials of the nitrogen molecule ($E°$ in V)

the *a*-axis is hindered, suggesting more difficult exfoliation or destruction of the graphite [21].

Concentrated nitric acid as oxidant

The oxidation–reduction potential of nitric acid is 2.08 V. Whereas nitric acid itself is well known as a strong oxidant, the standard potentials of several other nitrogen-containing compounds shown in Scheme 1, including some partial decomposition products of nitric acid, are also above 1.5 V. In addition, when its solution is heated, its oxidation capability will increase further. Consequently, it is thought that nitric acid solution may act as an oxidant to modify natural graphite like the solution of $(NH_4)_2S_2O_8$ [22].

A comparison of the electrochemical properties of virgin natural graphite A and the oxidized samples N1, N2, and N3 is shown in Fig. 7. The reversible capacity of the oxidized natural graphite increased to 335 mAh/g, the coulombic efficiency in the first cycle was as high as 88%, and there was no evident fading of reversible capacity in the first 10 cycles independently of the applied treatment temperature. This clearly suggests that concentrated nitric acid can also act as an efficient oxidant to modify natural graphite.

Green oxidants

Treatment with the strong oxidants discussed above will leave some environmentally undesirable chemicals which can be recovered in part through additional efforts. Even more attractive are processes leaving no unfriendly remains at all. Thus ''green chemistry'' has moved into the focus of current research efforts.

Oxidation–reduction potentials of aqueous solutions of hydrogen peroxide and ceric sulfate are 1.78 V and 1.61 V, respectively; they are between those of $(NH_4)_2S_2O_8$ and HNO_3. In addition, they can be easily recovered by electrolysis. If they are successfully applied to the improvement of the electrochemical performance of natural graphite, these ''green methods'' might be commercialized [23].

Electrochemical properties of virginal natural graphite A and the oxidized samples A1 and A2 are shown in Fig. 8. Evidently the electrochemical performance of the modified natural graphite is also markedly improved. The reversible capacity, coulombic efficiency in the first cycle, and cycling behavior are suitable for lithium ion batteries. This suggests that green methods can be adopted to modify common natural graphite as an anode material for lithium ion batteries.

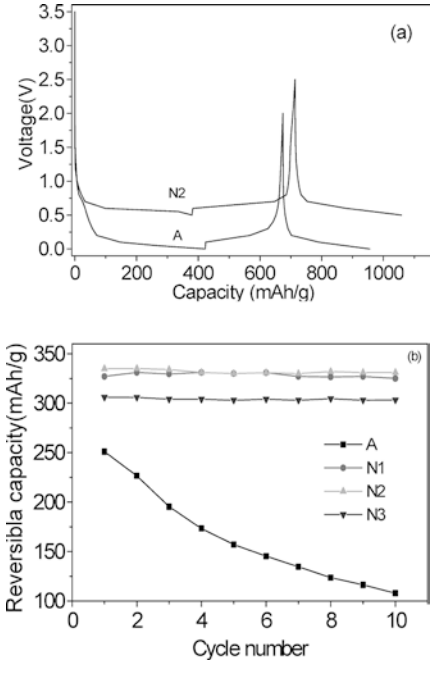

Fig. 7 (**a**) Discharge and charge profiles in the first cycle and discharge profiles in the second cycle of natural graphite A and the prepared sample N2 and (**b**) cycling behavior of virginal natural graphite and the prepared samples N1, N2, and N3 (in **a**, the voltages of N2 are shifted upwards by 0.5 V for clarity)

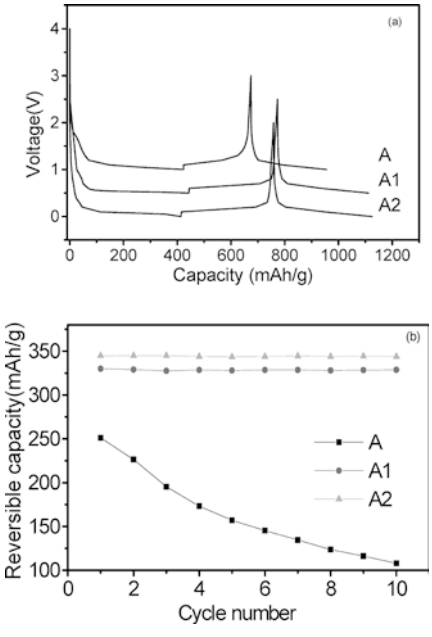

Fig. 8 (**a**) Discharge and charge profiles in the first cycle and discharge profiles in the second cycle and (**b**) cycling behavior of natural graphite A and the prepared samples A1 and A2 (in **a**, the voltages of A1 and A are shifted upwards by 0.5 and 1.0 V, respectively, for clarity)

Conclusion

Liquid/solid phase oxidation by solutions of ammonium peroxosulfate, nitric acid, and green oxidants (solutions of hydrogen peroxide and ceric sulfate) can modify natural graphite, resulting in good electrochemical performance as an anode material for lithium ion batteries. Oxidation removes active defects in natural graphite, forms a new dense film consisting of oxides, improves the stability, and introduces more nanochannels/micropores. These modifications inhibit the decomposition of electrolytes, prevent the movement of graphene molecules along *a*-axis direction, and provide more passages and storage sites for lithium. As a result, coulombic efficiency in the first cycle increases, reversible capacity enhances, and cycling behavior improves. The oxidation is performed under mild conditions, and the uniformity of the products can be well controlled.

In a pilot plant, we used a solution of ammonium peroxosulfate as an oxidant to modify natural graphite. It is easily processed, the product is uniform, and the costs are low. The electrochemical performance, including reversible capacity and cycling behavior of the assembled lithium ion battery, which used $LiCoO_2$ as the cathode, is also very good. This shows promise of these methods for industry.

Acknowledgements Financial support from the China Postdoctor Foundation and the Alexander von Humboldt Foundation is greatly appreciated.

References

1. Wu YP, Wan C, Jiang C, Fang SB (2002) Introduction, principles and advances of lithium secondary batteries. Tsinghua University Press, Beijing
2. Besenhard JO (1999) Handbook of battery materials. Wiley-VCH, Weinheim
3. Hossain S, Saleh Y, Loutfy R (2001) J Power Sources 96:5
4. Nakajima T, Yanagida K (1996) Tanso 174:195
5. Yoshio M, Wang H, Fukuda K, Hara Y, Adachi Y (2000) J Electrochem Soc 147:1245
6. Menachem C, Wang Y, Floners J, Peled E, Greenbaum SG (1998) J Power Sources 76:180
7. Wu YP, Jiang C, Wan C, Tsuchida E (2000) Electrochem Commun 2:626
8. Zaghib K, Nadeau G, Guerfi A, Brochu F (2000) ITE Lett Batteries, New Technol Med 1:892
9. Wang H, Yoshio M (2001) J Power Sources 93:123
10. Kim S, Kadoma Y, Ikuma H, Uchimoto Y, Wakihara M (2001) Electrochem Solid-State Lett 4:A109
11. Buqa H, Golob P, Winter M, Bensenhard JO (2001) J Power Sources 97–98:122
12. Wu YP, Jiang C, Wan C, Li J, Li Y (2000) Chin J Batteries 30:143
13. Wu YP, Jiang C, Wan C, Tsuchida E (2000) Electrochem Commun 2:272
14. Blackman L (1970) Modern aspects of graphite technology. Academic Press, London
15. Chung GC, Jun SH, Lee KY, Kim MH (1999) J Electrochem Soc 146:1664
16. Wu Z, Pittman CU (1995) Carbon 33:597
17. Zielke U, Huttinger KJ, Hoffman WP (1996) Carbon 34:983
18. Moreno-Castilla C, Ferro-Garcia MA, Joly JP, Bautista-Toledo I, Carrasco-Marin F, Rivera-Utrilla J (1995) Langmuir 11:4386
19. Wu YP, Wan C, Jiang C, Fang SB, Jiang YY (1999) Carbon 37:1901
20. Mabuchi A, Katsuhisa T, Fujimoto H, Kasuh T (1995) J Electrochem Soc 142:1041
21. Wu YP, Jiang C, Wan C, Holze R (2003) J Appl Electrochem (in press)
22. Wu YP, Jiang C, Wan C, Holze R (2003) J Power Sources (in press)
23. Wu YP, Jiang C, Wan C, Tsuchida E (2001) J Mater Chem 11:1233